Differential requirement for BMP signaling in atrial and ventricular lineages establishes cardiac chamber proportionality

Sara R. Marques [a,b], Deborah Yelon [a,*]

[a] Developmental Genetics Program and Department of Cell Biology, Kimmel Center for Biology and Medicine, Skirball Institute of Biomolecular Medicine, New York University School of Medicine, New York, NY 10016, USA
[b] Graduate Program in Areas of Basic and Applied Biology, Universidade do Porto, 4050-465 Porto, Portugal

ABSTRACT

The function of an organ relies upon the proper relative proportions of its individual operational components. For example, effective embryonic circulation requires the appropriate relative sizes of each of the distinct pumps created by the atrial and ventricular cardiac chambers. Although the differences between atrial and ventricular cardiomyocytes are well established, little is known about the mechanisms regulating production of proportional numbers of each cell type. We find that mutation of the zebrafish type I BMP receptor gene *alk8* causes reduction of atrial size without affecting the ventricle. Loss of atrial tissue is evident in the lateral mesoderm prior to heart tube formation and results from the inhibition of BMP signaling during cardiac progenitor specification stages. Comparison of the effects of decreased and increased BMP signaling further demonstrates that atrial cardiomyocyte production correlates with levels of BMP signaling while ventricular cardiomyocyte production is less susceptible to manipulation of BMP signaling. Additionally, mosaic analysis provides evidence for a cell-autonomous requirement for BMP signaling during cardiomyocyte formation and chamber fate assignment. Together, our studies uncover a new role for BMP signaling in the regulation of chamber size, supporting a model in which differential reception of cardiac inductive signals establishes chamber proportion.

© 2009 Elsevier Inc. All rights reserved.

Introduction

Organ function is the cumulative effect of coordinating each of an organ's individual subunits. In the vertebrate heart, the propulsion of circulation depends upon the serial contraction of each of its independent pumps, the atrial and ventricular cardiac chambers. Therefore, attainment of proper cardiac chamber proportionality is crucial for effective cardiac function.

Little is known about the mechanisms that regulate the relative sizes of the cardiac chambers. Atrial and ventricular cardiomyocytes are distinct cell types that differ both histologically and physiologically (Moorman and Christoffels, 2003). For example, in the zebrafish heart tube, chamber cardiomyocytes have distinct cell morphologies, with atrial cardiomyocytes appearing more squamous and ventricular cardiomyocytes appearing more cuboidal (Rohr et al., 2008). Additionally, zebrafish atrial and ventricular cardiomyocytes express the chamber-specific myosin heavy chains, *atrial myosin heavy chain* (*amhc*) and *ventricular myosin heavy chain* (*vmhc*) (Berdougo et al., 2003; Yelon et al., 1999). Although several transcription factors have been implicated in the regulation of chamber-specific characteristics (Bruneau, 2002), the signaling pathways that trigger initial chamber

fate assignment and generate the appropriate numbers of atrial and ventricular cardiomyocytes are poorly understood.

Analysis of the mechanisms regulating chamber size is relatively convenient in the simple two-chambered zebrafish heart, in contrast to the four-chambered mammalian heart, which arises from multiple heart fields (Buckingham et al., 2005; Cai et al., 2003; Kelly et al., 2001; Meilhac et al., 2004). Fate map experiments in zebrafish reveal that cardiac progenitors are located at the lateral margin of the embryo at the onset of gastrulation (Keegan et al., 2004). Even at this early stage, chamber progenitor populations are already spatially organized. Within the lateral marginal zone of the blastula, atrial progenitors are located more ventrally, and ventricular progenitors are located more dorsally; additionally, ventricular progenitors tend to be closer to the margin than are the atrial progenitors (Keegan et al., 2004). The relative organization of chamber progenitors seems to be maintained during and after gastrulation (Keegan et al., 2004; Schoenebeck et al., 2007). Cardiac specification is thought to take place during the time window in which the migrating progenitor cells form the lateral plate mesoderm, culminating in robust expression of precardiac markers like *nkx2.5* around the 6–8 somite stage (Thomas et al., 2008). Myocardial differentiation then initiates around the 13–14 somite stage (Yelon et al., 1999), and chamber-specific gene expression is first evident at the 14 somite stage with the expression of *vmhc* (Yelon et al., 1999) and at the 19 somite stage with the expression of *amhc* (Berdougo et al., 2003).

* Corresponding author. Fax: +1 212 263 7760.
  E-mail address: yelon@saturn.med.nyu.edu (D. Yelon).

Recent work in zebrafish supports an emerging idea regarding the acquisition of chamber identity: the signals responsible for cardiac induction may also be responsible for the subdivision of the heart field into atrial and ventricular territories. These studies demonstrated that mild inhibition of cardiac inductive signals can lead to differential reduction of atrial and ventricular chambers. For example, although complete inhibition of Nodal signaling eliminates all cardiac mesoderm (Gritsman et al., 1999), modest loss of Nodal signaling results in reduced heart size with a particularly striking reduction of the ventricle (Reiter et al., 2001). Fate mapping experiments revealed that Nodal promotes ventricular fate assignment in blastomeres nearest to the margin (Keegan et al., 2004), consistent with a vegetal–animal gradient of Nodal signaling that positions the highest levels of Nodal signaling closest to the margin (Chen and Schier, 2002). A similar trend is observed in experiments inhibiting the FGF signaling pathway, which has also been implicated in promoting cardiac induction (Dunwoodie, 2007). Zebrafish *fgf8* mutants form small hearts with disproportionately small ventricles (Reifers et al., 2000), and temporal inhibition of FGF signaling has demonstrated its particular importance for ventricular cardiomyocyte formation during gastrulation stages (Marques et al., 2008), consistent with a dorsal–ventral gradient of FGF signaling that correlates with the more dorsal location of ventricular progenitors (Fürthauer et al., 1997; Keegan et al., 2004). Together, these studies suggest that differential reception of cardiac inductive signals within a uniform pool of cardiac progenitors could dictate chamber identity assignment.

BMP signaling has a conserved role in cardiac induction (Zaffran and Frasch, 2002). In *Drosophila*, *dpp* mutant embryos lack expression of *tinman*, an essential cardiac transcription factor gene, and do not form a dorsal vessel (Frasch, 1995). Conversely, ectopic Dpp can induce formation of ectopic *tinman*-expressing cells (Yin and Frasch, 1998). In chick, exogenous application of BMP also induces expression of the *tinman* homolog *NKX2-5* (Nakajima et al., 2002; Schlange et al., 2000; Schultheiss et al., 1997). Additionally, excess BMP signaling in mouse *Nkx2-5* mutants is thought to be responsible for the overspecification of cardiac progenitors (Prall et al., 2007). As in *Drosophila*, severe loss of cardiac tissue is also observed when BMP signaling is inhibited in vertebrates. In frog, inhibition of BMP signaling results in the absence of a morphologically recognizable heart (Shi et al., 2000). In mouse *Bmp2* mutants, expression of *Nkx2-5* is reduced or absent (Zhang and Bradley, 1996), and conditional removal of *Bmpr1* from precardiac mesoderm with a *Mesp-1 Cre* driver dramatically reduces the heart field (Klaus et al., 2007). Similarly, zebrafish *swirl* (*bmp2b*) mutants lack expression of *nkx2.5* (Kishimoto et al., 1997; Nguyen et al., 1998; Reiter et al., 2001).

While strong reduction of BMP signaling severely compromises heart development, mild reduction results in formation of a dysmorphic heart (Chocron et al., 2007). Zebrafish *lost-a-fin* (*laf*) mutants exhibit a weak dorsalized phenotype characterized by loss of the ventral tail fin, due to disruption of the type I BMP receptor gene *alk8* (Bauer et al., 2001; Mintzer et al., 2001). Maternal–zygotic *laf* mutants are morphologically similar to *swirl* (Mintzer et al., 2001). In contrast to the dramatic loss of cardiac tissue observed in *swirl* mutants, zygotic *laf* mutants form hearts with abnormal atrial morphology (Chocron et al., 2007). Because of the correlation between the relatively ventral location of atrial progenitors and the ventral–dorsal gradient of BMP signaling during gastrulation stages (Tucker et al., 2008), we hypothesized that the abnormal atrial morphology in *laf* mutants could reflect a role for BMP in atrial cardiomyocyte generation.

Here, we analyze the effects of BMP signaling on cardiac chamber size in the zebrafish embryo. We find that *laf* mutants exhibit a significant reduction in the number of atrial cardiomyocytes. Atrial tissue reduction occurs before the heart tube forms and results from inhibition of BMP signaling during cardiac progenitor specification stages. Conversely, high levels of BMP signaling result in a preferential increase of atrial size. Through mosaic analysis, we

show that BMP signaling is cell autonomously required for cardiomyocyte formation and chamber identity acquisition. Together, our data reveal a crucial role for BMP signaling in regulating cardiac chamber proportion through differential effects on atrial and ventricular progenitor populations.

Materials and methods

Zebrafish

We employed the following zebrafish mutations and transgenes: *lost-a-fin*^{sk42} (*laf/alk8*), *Tg(cmlc2:DsRed2-nuc)*^{f2} (Mably et al., 2003), *Tg(cmlc2:egfp)*^{twu277} (Huang et al., 2003) and *Tg(hsp701:dnBmpr-GFP)*^{w30} (Pyati et al., 2005). The *laf*^{sk42} mutation is a recessive lethal allele that was identified in a screen for ethylnitrosourea-induced mutations that affect cardiac chamber morphology (Auman et al., 2007). *laf*^{sk42} fails to complement *laf*^{tm110b}, and the phenotypes of *laf*^{sk42} and *laf*^{tm110b} mutants appear indistinguishable (Bauer et al., 2001; Chocron et al., 2007; Mintzer et al., 2001; Mullins et al., 1996). All zebrafish work followed protocols approved by the NYU School of Medicine IACUC.

Immunofluorescence and cell counting

We counted cardiomyocytes in embryos carrying the transgene *Tg(cmlc2:DsRed2-nuc)*, using immunofluorescence to detect DsRed in cardiomyocyte nuclei and to detect atrial myosin heavy chain (Amhc) in atrial cells, as described previously (Marques et al., 2008). Student's *t*-test (homocedastic, two-tail distribution) was used to analyze the differences between the means of cell number data sets.

In situ hybridization

Anti-sense probes for *amhc*, *vmhc*, *nkx2.5*, *hand2*, and *gata5* were used as previously described for in situ hybridization (Berdougo et al., 2003; Chen and Fishman, 1996; Reiter et al., 2001; Yelon et al., 1999, 2000).

Dorsomorphin treatments

A 10 mM stock of dorsomorphin (Calbiochem, #171261) in DMSO was diluted to a working concentration of 5 μM in E3 medium (Nusslein-Volhard and Dahm, 2002), a concentration previously described to cause dorsalization (Yu et al., 2008). Up to 10 embryos were treated in a final volume of 1 mL in a glass vial. Vials were kept on a nutator in the dark at 28.5 °C. Control embryos were treated with a corresponding dilution of DMSO.

Heat shock conditions

Embryos from outcrosses of fish heterozygous for *Tg(hsp701:dnBmpr-GFP)* were exposed to heat shock at desired stages through placement in 40 mL of embryo medium in a Petri dish on top of a covered heat block for 1 h at 37 °C. Following heat shock, transgenic embryos were identified by *gfp* expression and body morphology. Transgenic embryos heat shocked during gastrulation exhibit a previously described mild dorsalization, while embryos heat shocked at the 8-somite stage are grossly comparable to wild-type (Pyati et al., 2005, 2006).

RNA injections

alk8CA and *alk8(K232R)* mRNAs were in vitro transcribed from previously described plasmids using the SP6 mMessage mMachine System (Ambion) (Bauer et al., 2001). Embryos were injected at the 1-cell stage with 15 pg of *alk8CA* mRNA or 20 pg of *alk8(K232R)* mRNA. Injection of either mRNA causes a range of phenotypes;
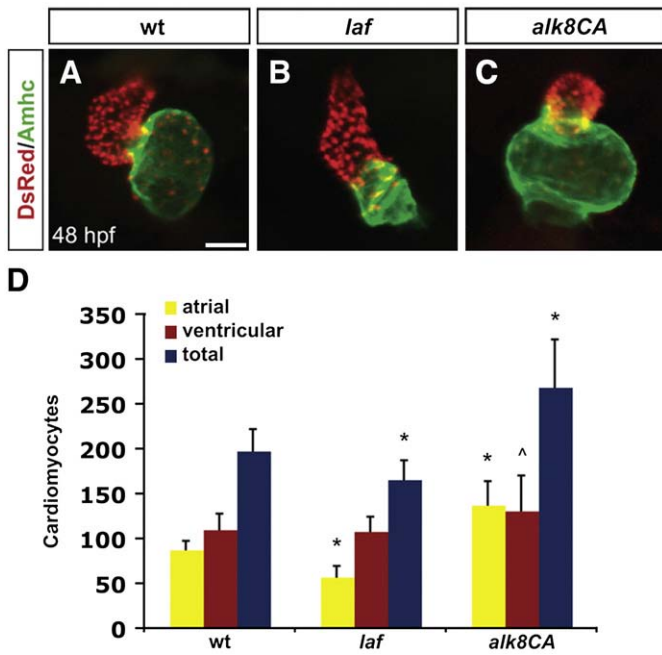
Fig. 1. Alk8 function regulates chamber proportionality. (A–C) Frontal views of hearts from wild-type (A), *laf* mutant (B) and *alk8CA* mRNA-injected (C) embryos at 48 h.p.f. Scale bar represents 50 µm. Immunofluorescence detects DsRed (red) in all cardiomyocyte nuclei and atrial myosin heavy chain (Amhc; green) in atrial cells. (A) In a wild-type heart, the ventricle (red) and atrium (green) exhibit typical looping and expansion. (B) In a *laf* mutant heart, the chambers are unlooped and dysmorphic. (C) In *alk8CA* mRNA-injected embryos displaying a v2–v3 class of ventralized body morphology (Kishimoto et al., 1997), the hearts are enlarged with a particularly striking expansion of the atrium. (D) Quantification of cardiomyocyte number in wild-type, *laf* mutant and *alk8CA* mRNA-injected embryos at 48 h.p.f. Graph indicates the mean and standard deviation for each data set; see also Table S1. Statistically significant differences from wild-type are indicated by asterisks ($p < 0.005$) or carets ($p < 0.05$). $n = 29$ for wild-type, $n = 19$ for *laf* mutants, and $n = 10$ for *alk8CA* mRNA-injected embryos. *laf* mutants and *alk8CA* mRNA-injected embryos have disproportionately small or large atrial chambers, respectively.

embryos were sorted into categories according to previously described scales of ventralization and dorsalization (Kishimoto et al., 1997; Mullins et al., 1996).
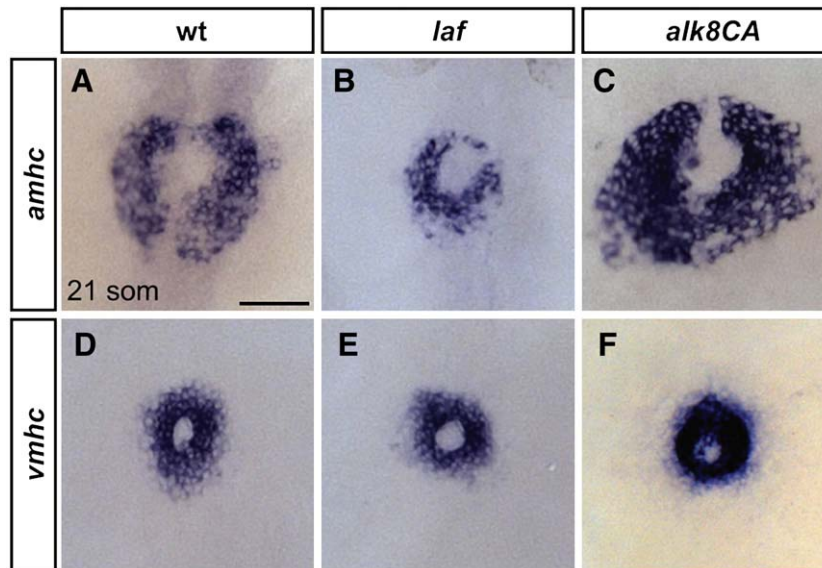
Transplantation

Transplantation was performed at midblastula stages as previously described (Ho and Kane, 1990; Parker and Stainier, 1999). 10–15 donor blastomeres were placed into the margin of a wild-type host embryo. Donor embryos carried either *Tg(cmlc2:egfp)* or fluorescein as a lineage tracer to allow detection of donor-derived cells in the host at 48 h post fertilization (h.p.f.). Donor embryos were either wild-type, injected with 1.5 pg of *alk8CA* mRNA, or injected with 2 ng of anti-*smad5* morpholino (5′-ATGGAGGTCATAGTGCTGGGCTGC-3′), the characterization of which will be described elsewhere (J.A. Tucker, V.H. Nguyen, A.P. Wiemelt, and M.C. Mullins, manuscript in preparation). At this concentration, the anti-*smad5* morpholino causes severe dorsalization without apparent nonspecific defects. Fisher's exact test was used to analyze the differences between frequencies of contribution to the myocardium.

Imaging

Images were captured with Zeiss Axioplan and M2Bio microscopes equipped with Zeiss Axiocam digital cameras and AxioVision software. Adobe Photoshop CS3 software was used to process images.

Results

Reduced atrial size in laf mutants

Prior studies of zebrafish *laf* (*alk8*) mutants have shown that loss of *laf* function results in formation of a linear, dysmorphic heart (Chocron et al., 2007). By 48 h.p.f., both the atrium and the ventricle are visibly misshapen in *laf* mutants (Figs. 1A, B). Quantification of the number of cardiomyocytes in each chamber reveals that the *laf* mutant atrium contains many fewer cardiomyocytes than the wild-type atrium (Fig. 1D), accounting for its shrunken appearance. In contrast, ventricular cell number is normal in *laf* mutants (Fig. 1D). The shortage of atrial cells in *laf* mutants is evident even prior to heart tube assembly (Figs. 2A, B), as shown by the reduced number of cells expressing *amhc*. Consistent with ventricular size at 48 h.p.f., expression of *vmhc* is relatively normal at earlier stages in *laf* mutants (Figs. 2D, E). The diminished population of atrial cardiomyocytes in *laf* mutants implicates BMP signaling in the regulation of atrial chamber size.

Fig. 2. Alk8 function impacts atrial cell number prior to heart tube formation. (A–F) In situ hybridization depicts expression of *amhc* (A–C) and *vmhc* (D–F) at the 21-somite stage; dorsal views, anterior to the top. Scale bar represents 50 µm. (A) In wild-type embryos, *amhc* is expressed in a ring of atrial cardiomyocytes just prior to heart tube extension, whereas in *laf* mutant embryos (B), the population of *amhc*-expressing cells is clearly reduced ($n = 14/15$). (C) In *alk8CA* mRNA-injected embryos displaying a v2–v3 ventralized body morphology, the population of *amhc*-expressing cells is clearly increased ($n = 20/23$). (D) *vmhc* is expressed in a ring of ventricular cardiomyocytes, located interior to the ring of atrial cardiomyocytes. The population of *vmhc*-expressing cells is comparable to wild-type in (E) *laf* mutants ($n = 14/14$) and seems slightly increased in (F) *alk8CA* mRNA-injected embryos ($n = 22/22$).

laf mutants exhibit lateral plate mesoderm deficiencies

The reduced number of atrial cells in *laf* mutants could be the consequence of an early defect in atrial progenitor specification or a later defect in atrial growth or differentiation. To determine whether the *laf* cardiac phenotype originates prior to myocardial differentiation, we examined molecular markers of cardiac progenitor populations in the anterior lateral plate mesoderm (ALPM) at the 10-somite stage. At this stage, cardiac progenitors reside within the *hand2* expression domain of the ALPM, with ventricular progenitors occupying a more medial territory defined by *nkx2.5* expression and atrial progenitors occupying a more lateral territory that does not yet express *nkx2.5* (Fig. 3A) (Schoenebeck et al., 2007). In keeping with previous reports (Chocron et al., 2007; Hogan et al., 2006), we find that *nkx2.5* expression in *laf* mutants is comparable to that seen in wild-type embryos (Figs. 3B,E). However, the *hand2* expression domain is considerably narrower in *laf* mutants (Figs. 3C, F). Likewise, *gata5* expression, which is normally expressed throughout the ALPM (Schoenebeck et al., 2007), appears in thinner strips of this tissue in *laf* mutants (Figs. 3D, G). Together, these expression patterns point to a defect in the width of the *laf* mutant ALPM, which also appears abnormally thin when visualized using Nomarski optics (SRM and DY, unpublished data). Moreover, the normal width of *nkx2.5* expression in *laf* mutants suggests that the missing portion of the LPM may be a lateral portion of the heart field, which normally contains atrial progenitors. Thus, *laf* function seems to influence formation of the atrial lineage from an early stage, well before myocardial differentiation begins.

BMP signaling is required during gastrulation stages to generate proper numbers of cardiomyocytes

Based on the *laf* ALPM phenotype, it seems likely that *bmp2*, *bmp4*, and *bmp7*, all of which are expressed during gastrulation on the ventral side of the embryo (Dick et al., 2000; Martínez-Barberá et al., 1997), could be involved in establishing appropriate atrial cell numbers. Alternatively, *bmp4* could also influence cardiac development at later stages, when it is expressed in the ALPM and cardiomyocytes (Martínez-Barberá et al., 1997). To confirm the importance of BMP signaling prior to myocardial differentiation, we temporally inhibited signaling using dorsomorphin, a pharmacological inhibitor of type I BMP receptors (Yu et al., 2008). Consistent with previous studies (Yu et al., 2008), we found that exposure to 5 μM dorsomorphin from 50%

epiboly onward results in the loss of ventral tail fin (Figs. 4A, B), mimicking the *laf* phenotype (Bauer et al., 2001; Mintzer et al., 2001). This period of dorsomorphin exposure also results in a significant reduction of atrial cardiomyocyte number, without a significant change in ventricular cell number (Fig. 4D), again reminiscent of *laf* mutants (Fig. 1D). Dorsomorphin exposure from tailbud stage onward causes mild ventral tail fin defects (Fig. 4C) and cloaca defects (SRM and DY, unpublished data), consistent with previously described roles for BMP signaling (Pyati et al., 2006), but this treatment does not affect cardiomyocyte number (Fig. 4D). We obtained similar results with a different method of inhibiting BMP signaling, employing *Tg(hsp701: dnBmpr-GFP)* transgenic embryos that express a heat-inducible dominant negative form of Alk8 (Pyati et al., 2005). Heat shock at 65% epiboly causes loss of ventral tail fin (Pyati et al., 2005), as well as fewer atrial and ventricular cardiomyocytes, with a more striking deficit of atrial cells (Fig. 4E). However, heat shock at later stages did not have a significant impact on cardiomyocyte number (Fig. 4E). Thus, both pharmacological and genetic inhibition point to an early requirement for BMP signaling, during cardiac progenitor specification stages, in the generation of the proper numbers of cardiomyocytes.

Levels of BMP signaling affect cardiomyocyte number and proportion in a dose-dependent manner

Throughout gastrulation stages, a steep ventral to dorsal gradient of BMP signaling is present in the zebrafish embryo and can be visualized by the spatial distribution of BMP ligands and phosphorylated Smad5, a transcription factor activated by activation of Alk8 (Bauer et al., 2001; Hild et al., 1999; Martínez-Barberá et al., 1997; Mintzer et al., 2001; Tucker et al., 2008). Therefore, the relatively ventral atrial progenitors are likely to be exposed to higher levels of BMP signaling than are the more dorsal ventricular progenitors, suggesting that differential levels of BMP signaling could affect chamber progenitor specification.

To test whether increased levels of BMP signaling could result in atrial population expansion, we injected embryos with mRNA encoding a constitutively active form of Alk8 (*alk8CA*), which is able to signal independently of ligand and type II receptor (Bauer et al., 2001; Wieser et al., 1995). Injection of *alk8CA* mRNA creates a range of phenotypes, ranging from highly ventralized to relatively normal body morphologies (Bauer et al., 2001). The most ventralized class of injected embryos (the v2–v3 class, according to a previously
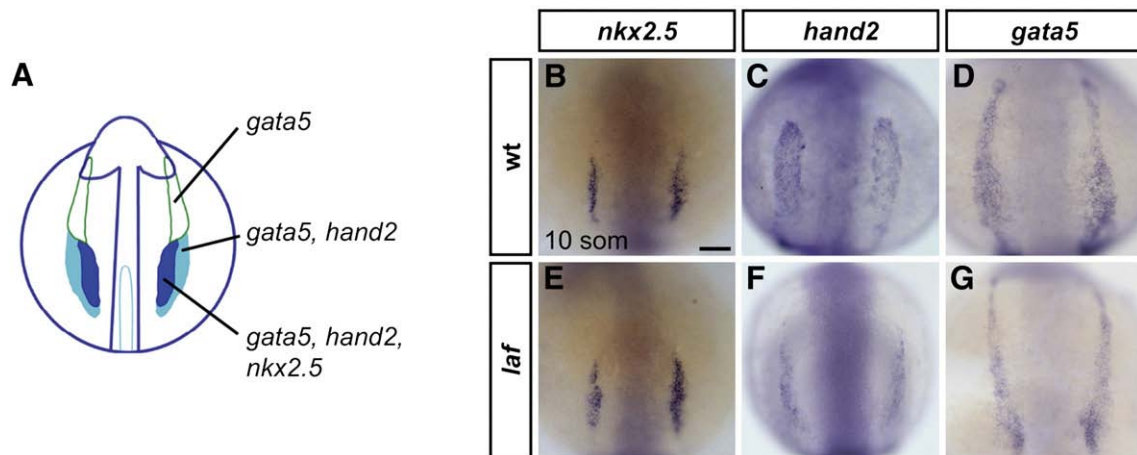

Fig. 3. *laf* mutants exhibit lateral plate mesoderm deficiencies. (A) Schematic representation of gene expression patterns in the ALPM in an embryo at the 10-somite stage (Schoenebeck et al., 2007); dorsal view, anterior to the top. *gata5* is expressed throughout the two bilateral strips of ALPM. *hand2* overlaps with *gata5* in the posterior regions of the ALPM, which correspond to the heart fields. *nkx2.5* overlaps with *hand2* in the medial portions of the heart fields. (B–G) In situ hybridization depicts expression of *nkx2.5*, *hand2* and *gata5* at the 10-somite stage; dorsal views, anterior to the top. Scale bar represents 50 μm. (B–D) are wild-type embryos and (E–G) are *laf* mutant siblings. (B, E) *nkx2.5* expression is indistinguishable in wild-type and *laf* mutant embryos ($n = 15/15$). (C, D, F, G) *laf* mutants display narrowed domains of *hand2* ($n = 18/20$) and *gata5* ($n = 17/20$) expression, revealing a defect in the width of the cardiac ALPM. *hand2* and *gata5* expression levels vary from normal to reduced in *laf* mutants, which also exhibit reduced expression of other cardiac progenitor markers, including *gata4*, *nkx2.7*, and *tbx5* (SRM and DY, unpublished data).
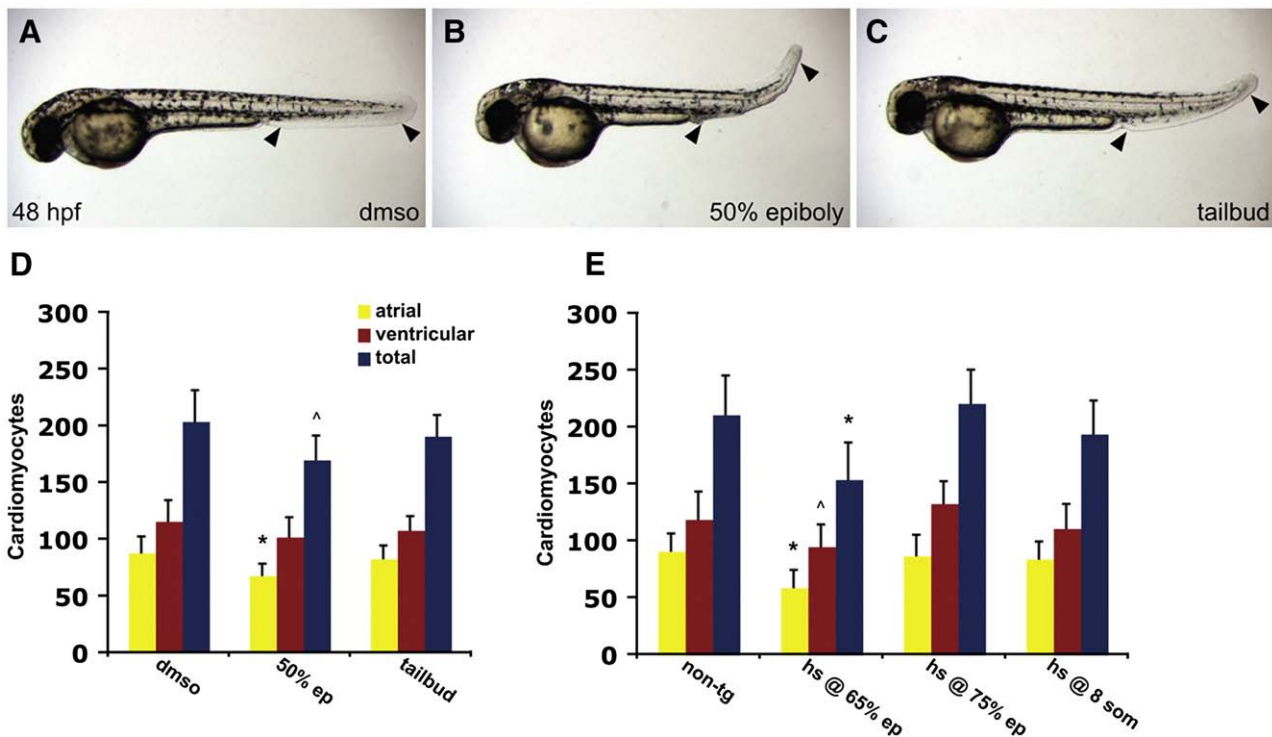
Fig. 4. Inhibition of BMP signaling during gastrulation results in decreased cardiomyocyte numbers. (A–C) Lateral views of embryos exposed to dorsomorphin from 50% epiboly (B) or tailbud (C) stages until 48 h.p.f.; all images are at the same magnification. (B) Embryos treated with dorsomorphin from 50% epiboly onward lack the ventral tail fin (arrowheads), phenocopying the *laf* mutant body morphology. (C) Embryos treated with dorsomorphin from tailbud stage onward display mild abnormalities of the ventral tail fin (arrowheads), which is smaller in comparison to control embryos (A, arrowheads) treated with the same concentration of DMSO. (D) Quantification of cardiomyocyte number at 48 h.p.f. following dorsomorphin treatment. Graph as in Fig. 1; see also Table S2. $n = 10$ for control DMSO treatment, $n = 10$ for 50% epiboly treatment, $n = 11$ for tailbud treatment. (E) Quantification of cardiomyocyte number at 48 h.p.f., following heat shock of embryos carrying the transgene *Tg(hsp701:dnBmpr-GFP)*. Control embryos were non-transgenic siblings, and heat shocks were performed at 65% epiboly, 75% epiboly, and the 8-somite stage. Graph as in Fig. 1; see also Table S3. $n = 18$ for non-transgenic embryos, $n = 14$ for heat shock at 65% epiboly, $n = 17$ for heat shock at 75% epiboly, and $n = 17$ for heat shock at the 8-somite stage. Statistically significant differences from wild-type are indicated by asterisks ($p < 0.005$) or carets ($p < 0.05$). Differences observed between the effects of dorsomorphin exposure and heat shock may be explained by differences in the strength of inhibition provided by each method.

described system of phenotypic classification; Kishimoto et al., 1997) display an enlarged atrium, with a large surplus of atrial cardiomyocytes as well as a slightly enhanced number of ventricular cardiomyocytes (Figs. 1C,D, 2C,F). Together with the *laf* mutant phenotype, these results suggest a correlation between levels of BMP signaling and atrial size.

To examine a broader spectrum of BMP signaling levels, we compared a diverse array of embryos injected with mRNA encoding either *alk8CA* or a dominant negative kinase dead form of Alk8 (*alk8 (K232R)*) (Bauer et al., 2001). Akin to the range of effects of *alk8CA* injection, *alk8(K232R)* mRNA injection creates a spectrum of dorsalized phenotypes (Bauer et al., 2001). We grouped both sets of injected embryos into previously described classes of ventralized or dorsalized body morphologies and quantified chamber cardiomyocyte number for each class (Fig. 5). The most ventralized embryos, characteristic of high levels of BMP signaling, displayed atrial enlargement (Figs. 1C, 5A), whereas the most dorsalized embryos, characteristic of low levels of BMP signaling, displayed small hearts (Fig. 5C). Comparing all classes of embryos, we find a correlation between level of BMP signaling and total cardiomyocyte number (Fig. 5D and Table 1). This positive correlation is also present for the number of atrial cardiomyocytes, which is significantly increased in the two most ventralized phenotypic classes, as opposed to the number of ventricular cardiomyocytes, which is not as enhanced in these embryos (Fig. 5D and Table 1). Likewise, antagonism of BMP signaling differentially affects the numbers of atrial and ventricular cardiomyocytes, with a stronger effect on the atrial population (Fig. 5D and Table 1). Thus, atrial size seems highly dependent on levels of BMP signaling, whereas the role of BMP signaling is less striking for the ventricle.

A cell-autonomous role for BMP signaling in cardiomyocyte formation

Our results suggest that BMP signaling plays an early role in promoting the acquisition of cardiac identity, particularly atrial identity. However, these data do not indicate whether BMP signaling plays a direct role in this regard. Recent work in mouse has shown that BMP signal reception is required within *Mesp-1*-expressing mesoderm for cardiomyocyte generation (Klaus et al., 2007). We wondered whether individual cardiac progenitors require direct reception of BMP signaling in order to acquire cardiac identity and whether the level of BMP signaling received impacts chamber identity choice. To address this, we performed blastomere transplantation to compare the contributions of wild-type cells and cells deficient in BMP signal transduction to the cardiac chambers of wild-type host embryos. To inhibit BMP signal transduction, we used a morpholino (MO) to interfere with Smad5 translation. Embryos injected with anti-*smad5* MO (*smad5* morphants) exhibit more severely dorsalized bodies and stronger cardiac phenotypes than those observed in *laf* mutants (SRM and DY, unpublished data). Donor-derived cardiomyocytes were recognizable in host embryos due to their expression of the transgene *Tg(cmlc2:egfp)* (Figs. 6A, B). In wild-type-into-wild-type control transplants, we found donor-derived cardiomyocytes in 13.2% of our experiments (15 out of 114 transplants) (Fig. 6C). Strikingly, in *smad5* morphant-into-wild-type transplants, donor-derived cells contributed to the myocardium much less frequently, becoming cardiomyocytes in only 1.2% of our experiments (2 out of 170 transplants), a significant difference from the effectiveness of wild-type donor cells (Fig. 6C). The poor ability of *smad5* morphant cells to contribute to the heart does not reflect a general problem with the viability of cells from morphant donors: both wild-
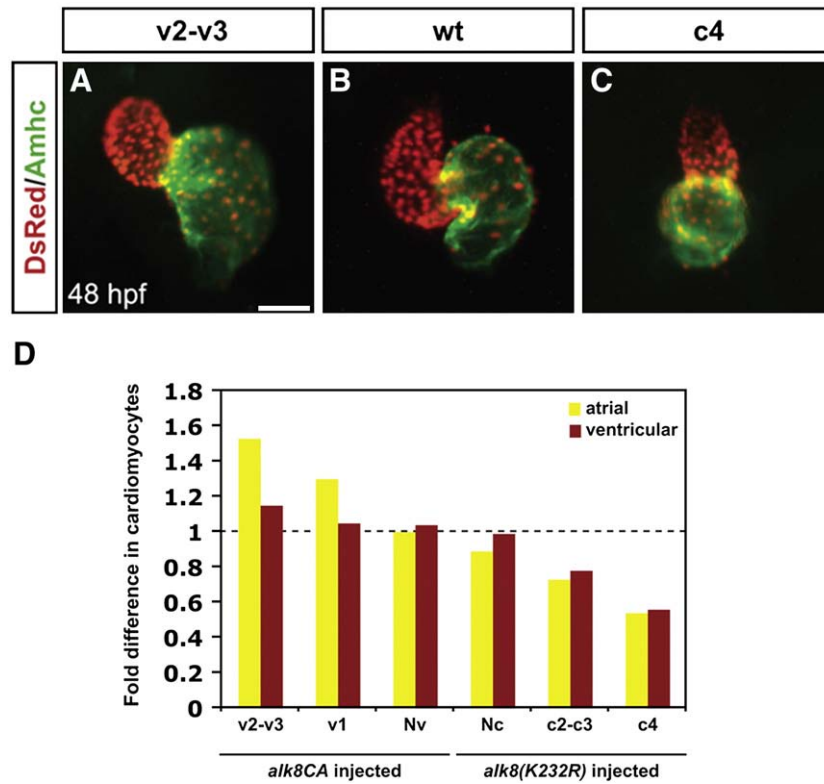
Fig. 5. Levels of BMP signaling affect cardiomyocyte number and proportion in a dose-dependent manner. (A–C) Frontal views of hearts at 48 h.p.f.; immunofluorescence as in Fig. 1. Scale bar represents 50 μm. Hearts depict examples from (A) an *alk8CA* mRNA-injected embryo displaying a v2–v3 class of severely ventralized body morphology (Kishimoto et al., 1997), (B) a wild-type embryo, and (C) an *alk8(K232R)* mRNA-injected embryo displaying a c4 class of severely dorsalized body morphology (Mullins et al., 1996). (D) Quantification of cardiomyocytes at 48 h.p.f., following injection of *alk8CA* or *alk8(K232R)* mRNA. Injected embryos were separated into previously described phenotypic classes based on body morphology. Injection of *alk8CA* mRNA causes a range of ventralization classes (v2–v3, v1, and Nv, meaning normal morphology) (Kishimoto et al., 1997). Injection of *alk8(K232R)* mRNA causes a range of dorsalization classes (Nc, meaning normal morphology, c2–c3 and c4) (Mullins et al., 1996). Graph indicates fold difference in mean values for each phenotypic class relative to wild-type embryos.

type and *smad5* morphant donor-derived cells contribute equally well to other tissues, such as skeletal muscle (Figs. 6D–F). Taken together, our results indicate that BMP signaling is required cell autonomously for cardiomyocyte formation.

A cell-autonomous role for BMP in chamber identity acquisition

Since cell-autonomous receipt of BMP signaling is crucial for the generation of cardiomyocytes (Figs. 6A–C), we could not use *smad5* morphant donors to evaluate conclusively whether BMP signal reception plays a cell-autonomous role during chamber fate assignment. Instead, we compared the contributions of wild-type cells and cells injected with *alk8CA* mRNA to the cardiac chambers of wild-type hosts. We first employed donor embryos injected with the same amount of *alk8CA* mRNA as in our other experiments (Figs. 1C, 2C, 2F, 5A). In these transplants, *alk8CA* mRNA-injected donor-derived

were very inefficient in contributing to the myocardium (1.6% contribution frequency; 2 out of 122 transplants), but contributed normally to skeletal muscle (75.6% contribution frequency; 31 out of 41 transplants). Together with our *smad5* morphant transplants, this result suggests that neither particularly high nor particularly low levels of BMP signaling allow donor-derived cells to become cardiomyocytes in the context of a wild-type host. Next, we injected donor embryos with a ten-fold lower concentration of *alk8CA* mRNA. In these transplants, *alk8CA* mRNA-injected donor-derived cells were more capable of contributing to myocardium (10.8% contribution frequency; 20 out of 185 transplants), closer to the effectiveness of wild-type cells (14.4% contribution frequency; 26 out of 181 transplants). If BMP signaling plays a cell-autonomous role in chamber identity acquisition, then we expected injection of this dose of *alk8CA* mRNA to affect the relative likelihood of donor-derived cells contributing to each chamber, favoring atrial over ventricular contributions. We found a significant

Table 1
Effects of altered BMP signaling on cardiomyocyte number and proportion

Class (n)	Atrial cell number	Ventricular cell number	Total cell number	Atrial fold diff.	Ventricular fold diff.	A/V ratio
v2–v3 (10)	*138 ± 39	^131 ± 26	*269 ± 53	1.53	1.14	1.05
v1 (12)	*117 ± 20	121 ± 19	*238 ± 30	1.3	1.05	0.97
Nv (11)	90 ± 11	119 ± 25	*209 ± 31	1	1.03	0.76
wt (13)	90 ± 10	115 ± 10	205 ± 18	1	1	0.78
Nc (9)	81 ± 16	113 ± 28	194 ± 37	0.9	0.98	0.72
c2–c3 (12)	*66 ± 22	^90 ± 36	*156 ± 52	0.73	0.78	0.73
c4 (7)	*48 ± 26	*64 ± 29	*112 ± 53	0.53	0.56	0.75

Values represent cardiac cell numbers (± standard deviation) and proportions for each phenotypic class following injection with either *alk8CA* or *alk8(K232R)* mRNA. Statistically significant differences from wild-type are indicated by asterisks (*p*<0.005) and carets (*p*<0.05).

Donor	Transplants with myocardial contribution	Total transplants	Myocardial contribution frequency
wt	15	114	13.2 %
smad5 MO	2	170	*1.2 %

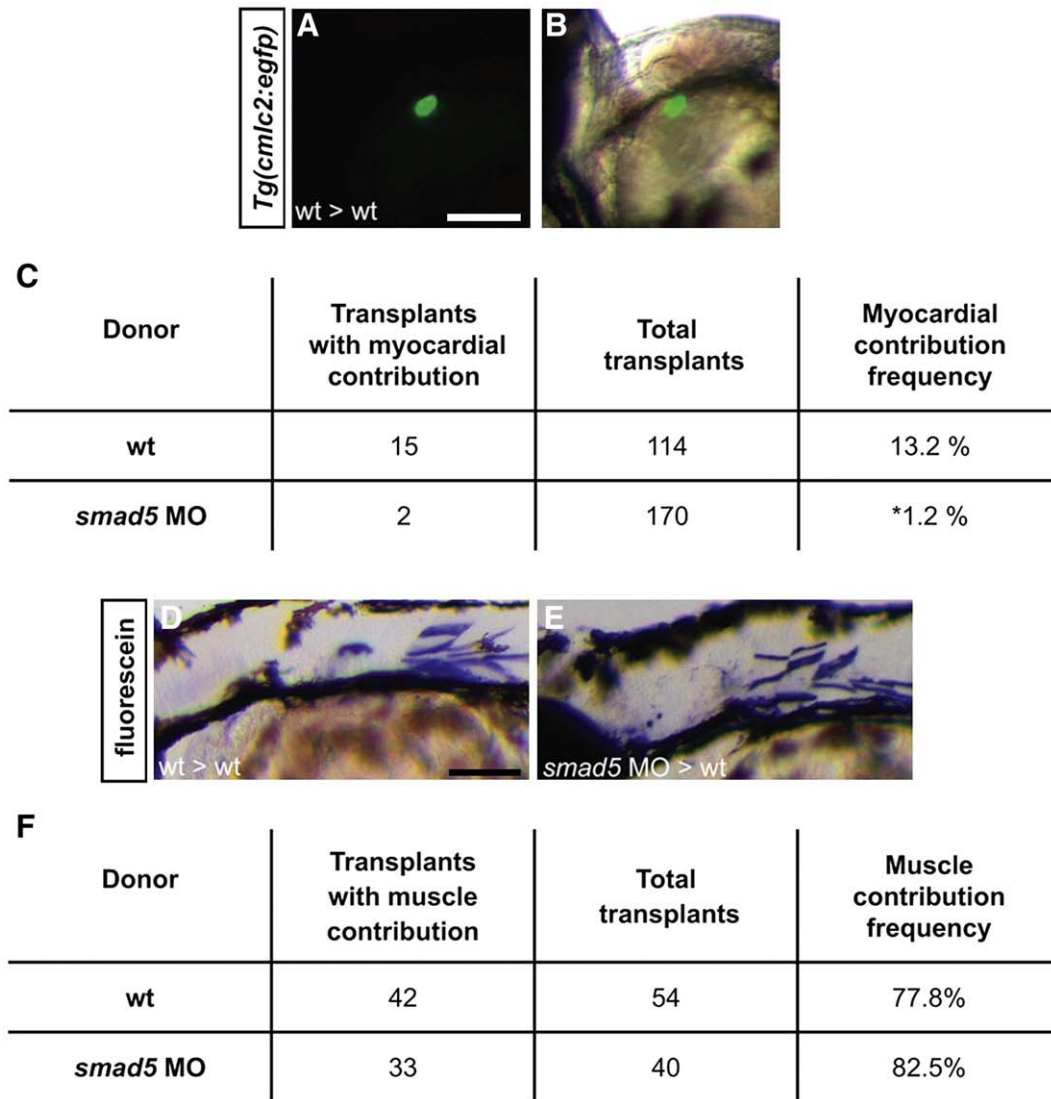| Donor	Transplants with muscle contribution	Total transplants	Muscle contribution frequency
wt	42	54	77.8%
smad5 MO	33	40	82.5%

Fig. 6. BMP signaling is required cell autonomously for cardiomyocyte formation. (A, B) Example of transplantation results; lateral views, ventral to the top, anterior to the left. (A) Wild-type donor-derived cells expressing Tg(cmlc2:egfp) in wild-type host myocardium at 48 h.p.f. Scale bars represent 50 μm. (B) Overlay of bright-field and fluorescent images revealing that the donor-derived cells are located in the outer curvature of the ventricle. (C) Table of transplantation results indicating the frequency of myocardial contribution of wild-type donor cells or smad5 morphant donor cells in wild-type host embryos. Cells from smad5 morphant donors contribute significantly less often to myocardium than do cells from wild-type donors; asterisk indicates p<0.05. In one example of smad5 morphant cardiomyocyte contributions, donor-derived cells were found in the ventricle; in the other example, donor-derived cells were found in both the atrium and the ventricle. (D, E) Detection of wild-type and smad5 morphant donor-derived cells in the skeletal muscle of wild-type host embryos at 48 h.p.f. by anti-fluorescein immunohistochemistry. Scale bars represents 50 μm. Lateral views, dorsal to the top, anterior to the left. (F) Table of transplantation results indicating the equivalent frequencies of skeletal muscle contribution of wild-type donor cells or smad5 morphant donor cells in wild-type host embryos. Differences between the frequency of wild-type contribution to myocardium and skeletal muscle are likely due to differences in organ field size. Since the skeletal muscle field is larger than the heart field (Kimmel et al., 1990), wild-type donor cells contribute to skeletal muscle more frequently.

difference in contribution to the ventricle, with alk8CA mRNA-injected cells contributing to the ventricle in only 5.9% of experiments (11 out of 185 transplants) and wild-type cells contributing to the ventricle in 12.2% of experiments (22 out of 181 transplants) (Fig. 7). In contrast, alk8CA mRNA-injected cells contributed to the atrium in 8.6% of experiments (16 out of 185 transplants), a subtle increase in contribution compared to that seen for wild-type cells, which contributed to the atrium in 6.6% of experiments (12 out of 181 transplants) (Fig. 7). Our data show that the likelihood of transplanted alk8CA mRNA-injected cells to contribute to one cardiac chamber or the other differs from the likelihood of wild-type contributions, indicating that the amount of BMP signaling received by transplanted cells affects their fate. Together, our data suggest that cell-autonomous receipt of BMP signaling influences chamber proportionality by biasing chamber fate assignment of progenitor cells.

Discussion

Our studies uncover a previously unrecognized role of BMP signaling in atrial development and provide a new perspective on the roles of BMP signaling during heart formation. In addition to their established roles as cardiac inductive signals, we show that BMPs are also essential for the generation of the appropriate relative numbers of atrial and ventricular cardiomyocytes. Manipulations of BMP signaling that cause aberrations in total cardiomyocyte number also cause distortion of the atrial/ventricular ratio, supporting a model in which both functions of BMP signaling occur simultaneously during gastrulation stages. We propose that receipt of BMP signals by aspiring cardiac progenitor cells promotes specification of their cardiac identity and also biases their chamber assignment, with higher levels of BMP signaling favoring atrial over ventricular fate.

A

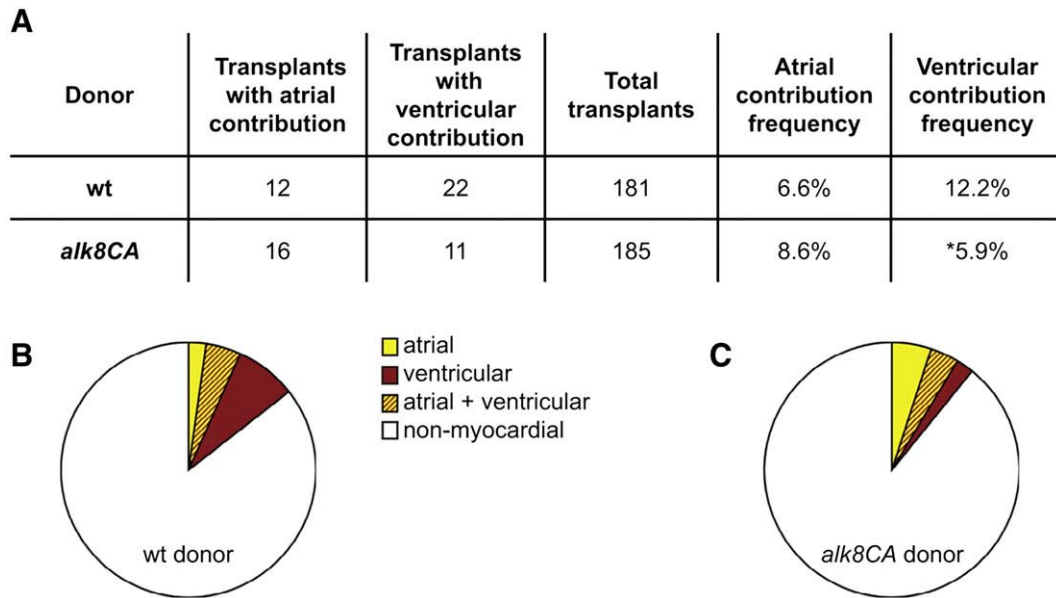| Donor	Transplants with atrial contribution	Transplants with ventricular contribution	Total transplants	Atrial contribution frequency	Ventricular contribution frequency
wt	12	22	181	6.6%	12.2%
alk8CA	16	11	185	8.6%	*5.9%

Fig. 7. BMP signaling plays a cell-autonomous role in determining chamber identity. (A) Table of transplantation results indicating the frequency of chamber contribution of wild-type donor cells or *alk8CA* mRNA-injected donor cells in wild-type host embryos. Cells from *alk8CA* mRNA-injected embryos have a slightly increased tendency to contribute to the atrium and contribute to the ventricle significantly less frequently than do wild-type cells; asterisk indicates $p < 0.05$. (B, C) Pie chart representations of contribution frequencies of wild-type (B) or *alk8CA* mRNA-injected (C) donor-derived cells in wild-type host embryos. Atrial (yellow), ventricular (red), atrial and ventricular (striped) and non-myocardial (white) contributions are indicated.

Thus, through differential effects on atrial and ventricular lineages, BMP signaling influences chamber size and thereby chamber proportionality.

The effect of BMP signaling on chamber fate assignment correlates nicely with the organization of myocardial progenitor cells within the lateral margin of the zebrafish blastula and its overlap with the described BMP signaling gradient. Within the lateral margin, Smad5 phosphorylation has been shown to be higher in the relatively ventral portion, which contains atrial progenitors, than it is in the relatively dorsal portion, which contains ventricular progenitors (Fig. 8A) (Keegan et al., 2004; Tucker et al., 2008). In a very simple model of how BMP might pattern the heart field, myocardial progenitors exposed to high levels of BMP signaling would become atrial progenitors, in parallel to the mechanism by which high levels of BMP signaling specify other ventral cell types (Kondo, 2007; Nguyen et al., 1998). Consistent with this model, we find that the atrial lineage is more susceptible than the ventricular lineage to both loss and gain of BMP signaling. This model would also predict that intermediate or low levels of BMP signaling would specify ventricular fate, in analogy to the role of BMP in specifying other lateral cell types (Nguyen et al., 1998; Stickney et al., 2007; Tucker et al., 2008). However, in our experiments, decreased levels of BMP signaling did not result in increased production of ventricular cardiomyocytes, and none of our alterations of BMP signaling provided results consistent with a fate transformation between atrial and ventricular lineages. Therefore, although BMP signaling has a potent influence on chamber proportionality, differential exposure to BMPs is not sufficient to pattern a uniform progenitor field into atrial and ventricular populations.

The lack of evidence for an atrial–ventricular fate transformation caused by manipulation of BMP signaling probably reflects the fundamental mechanism by which the cardiac progenitor lineages are separated. Instead of a uniform progenitor pool that is divided into two by differential reception of BMP signaling, we favor the notion of two separate progenitor pools with distinct requirements for BMP signaling (Fig. 8B). A shared pool model predicts that high BMP levels would substantially increase the atrial/ventricular ratio and that low BMP levels would substantially reduce it. However, our observed variations in proportionality are mild and do not support a

shared pool model. Furthermore, in highly dorsalized embryos, the atrial/ventricular ratio is closer to the wild-type ratio than to the ratio in *laf* mutants. Therefore, our observations are more consistent with a separate pools model. The atrial and ventricular lineages are already separate by midblastula stages (Keegan et al., 2004; Stainier et al., 1993), so the two progenitor pools may already have distinct requirements for BMP signaling. These pools would not only receive distinct amounts of BMP signaling but also differ in their responsiveness to BMP signaling. Since *alk8* and *smad* genes are expressed ubiquitously throughout gastrula stages (Dick et al., 1999; Müller et al., 1999; Yelick et al., 1998), the difference in responsiveness is not likely to be due to differences in these components of the BMP signaling pathway.

A separate pools model would also be consistent with our prior observations regarding the role of FGF signaling during chamber fate assignment (Marques et al., 2008). We have found that the ventricular lineage is more sensitive than the atrial lineage to loss of FGF signaling, correlating with the location of ventricular progenitors nearer to high levels of FGF signaling (Fürthauer et al., 1997; Keegan et al., 2004). However, low levels of FGF signaling do not result in increased production of atrial cardiomyocytes (Marques et al., 2008), again arguing against a shared pool model.

Together, our studies of BMP and FGF signaling suggest that chamber proportionality is established by a network of interacting pathways, which create a system buffered against the disruption of a single pathway. The BMP and FGF pathways are unlikely to be the only participants in this network, since chamber proportionality is not restored in *fgf8;alk8* double mutants (SRM and DY, unpublished data). In addition to other ventricularizing influences like the Nodal signaling pathway, the network could also include other atrializing influences, such as the retinoic acid (RA) signaling pathway, which has been suggested to specify atrial identity at the expense of ventricular identity in chick (Hochgreb et al., 2003; Xavier-Neto et al., 2001). However, recent studies in zebrafish indicate that a loss of RA signaling increases both atrial and ventricular populations, without evidence of a fate transformation between the lineages (Waxman et al., 2008). Further studies will be necessary to identify additional signaling pathways that interact with the BMP pathway during atrial fate assignment.
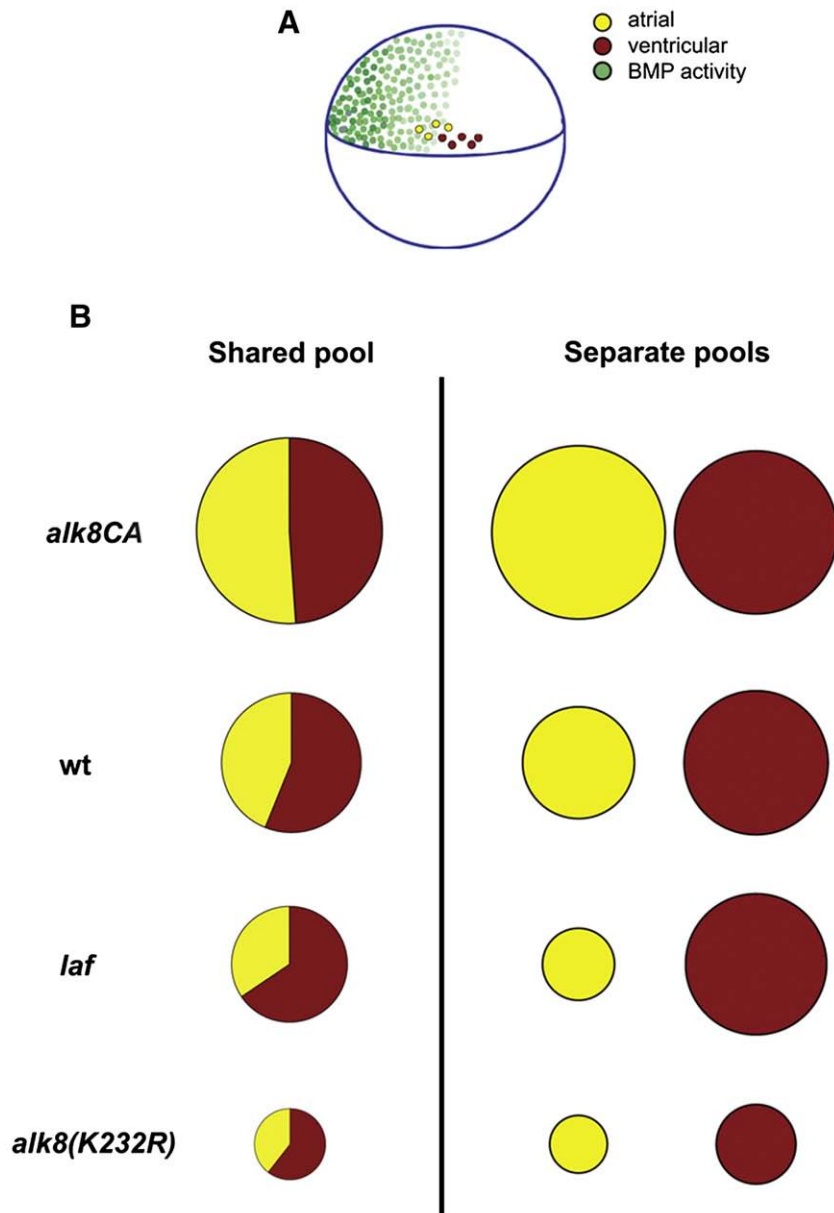
Fig. 8. The impact of BMP signaling on cardiac chamber fate assignment. (A) Cartoon represents the locations of ventricular (red) and atrial (yellow) progenitor cells relative to the locations of BMP signaling activity (green) at the onset of gastrulation, based on the established fate map and phospho-Smad5 distribution data (Keegan et al., 2004; Tucker et al., 2008). Lateral view, dorsal to the right. (B) Cartoons represent the impact of altering levels of BMP signaling on the size and proportion of the atrial (yellow) and ventricular (red) chamber progenitor pools. In the shared pool column, pie charts represent the presumed size and proportions of a shared cardiac progenitor pool that is divided into atrial and ventricular portions, based on our observations of cardiomyocyte numbers in wild-type, *laf* mutant, *alk8CA* mRNA-injected, and *alk8(K232R)* mRNA-injected embryos. In the separate pools column, circles represent the presumed relative sizes of each separate chamber progenitor pool, again based on our observations of cardiomyocyte numbers. In either model, it is clear that the atrial and ventricular lineages are differentially sensitive to the impact of BMP signaling.

Whether BMP signaling influences the choice between atrial and ventricular identities or the choice between cardiac and non-cardiac identities, it is clearly playing a direct role in the decisions made by cardiac progenitors. Because of the early requirement for BMP signaling and the early ALPM defects observed in *laf* mutants, we favor the notion that BMP signaling directly affects progenitor specification or migration into the ALPM. Although we cannot rule out the possibility that BMP signaling influences progenitor proliferation, it seems unlikely that BMP signaling regulates progenitor survival since we do not detect an increased number of apoptotic cells within the heart fields of *laf* mutants (SRM and DY, unpublished data). In future studies, it will be important to identify the downstream targets responsible for the effects of BMPs on chamber fate acquisition. These targets may be subsets of genes in

the myocardial differentiation program that dictate chamber identity, especially since Smad binding sites are known to modulate expression of precardiac genes like *Nkx2-5* in chick and mouse (Brown et al., 1998; Lee et al., 2004; Liberatore et al., 2002; Lien et al., 2002). Additionally, BMP targets might play important roles in directing the patterns of movement of progenitor cells as they create the heart fields in the ALPM. Abnormal migration of myocardial progenitors causes reduction of heart size (Scott et al., 2007; Zeng et al., 2007). During gastrulation, ventrally located BMP signals have a repulsive effect on lateral mesodermal cells, which fail to migrate dorsally in severely reduced BMP signaling scenarios (von der Hardt et al., 2007). Therefore, it is possible that the migration of the more ventral atrial progenitors into the ALPM is more affected by levels of BMP signaling than is the migration of ventricular progenitors.

Taken together, our results indicate that BMP signaling regulates heart size and chamber proportionality by differentially regulating atrial and ventricular cardiomyocyte number. Our data suggest a model in which BMP signaling regulates the acquisition of cardiac fate of separate pre-atrial and pre-ventricular pools, which behave similarly but differ in their sensitivity to BMP signaling. It is interesting to consider whether the role of BMP signaling in regulating chamber proportionality may be conserved in amniotes. Multiple studies have implicated BMP signaling at several developmental stages in distinct aspects of amniote heart development (van Wijk et al., 2007). During cardiac morphogenesis, it is clear that BMPs influence establishment of left–right asymmetry (Branford et al., 2000; Chocron et al., 2007; Mine et al., 2008; Smith et al., 2008), outflow tract morphogenesis (Délot et al., 2003; Liu et al., 2004; Stottmann et al., 2004), and valve formation (Délot et al., 2003; Liu et al., 2004; Solloway and Robertson, 1999; Sugi et al., 2004). At earlier stages, cardiac progenitors are clearly exposed to BMP signaling in both chick and mouse, as has been demonstrated in studies of the impact of BMPs on cardiac induction (Dunwoodie, 2007; Zaffran and Frasch, 2002). Although removal of BMP signaling has been shown to shrink or eliminate the mouse heart field (Klaus et al., 2007), it is not yet clear how BMPs impact chamber proportionality in mouse. More subtle manipulations of BMP signaling would be desirable for examination of this role. Analysis of chamber formation in amniotes is challenging due to the contributions of multiple myocardial lineages to the right ventricle and atria (Buckingham et al., 2005; Meilhac et al., 2004). Use of lineage-specific markers and tracers that distinguish between primary and secondary contributions to each chamber will help to determine the precise requirements for chamber identity acquisition in each amniote heart field. Such studies will be of great interest in the future, especially since the cell-autonomous impact of BMP signaling on chamber identity acquisition would be useful to harness for applications in regenerative medicine.

Acknowledgments

Appendix A. Supplementary data

Supplementary data associated with this article can be found, in the online version, at doi:10.1016/j.ydbio.2009.02.010.

References

Auman, H.J., Coleman, H., Riley, H.E., Olale, F., Tsai, H.J., Yelon, D., 2007. Functional modulation of cardiac form through regionally confined cell shape changes. PLoS Biol. 5, e53.

Bauer, H., Lele, Z., Rauch, G.J., Geisler, R., Hammerschmidt, M., 2001. The type I serine/ threonine kinase receptor Alk8/Lost-a-fin is required for Bmp2b/7 signal transduction during dorsoventral patterning of the zebrafish embryo. Development 128, 849–858.

Berdougo, E., Coleman, H., Lee, D.H., Stainier, D.Y., Yelon, D., 2003. Mutation of weak atrium/atrial myosin heavy chain disrupts atrial function and influences ventricular morphogenesis in zebrafish. Development 130, 6121–6129.

Branford, W.W., Essner, J.J., Yost, H.J., 2000. Regulation of gut and heart left–right asymmetry by context-dependent interactions between Xenopus lefty and BMP4 signaling. Dev. Biol. 223, 291–306.

Brown, L.A., Amores, A., Schilling, T.F., Jowett, T., Baert, J.L., de Launoit, Y., Sharrocks, A.D., 1998. Molecular characterization of the zebrafish PEA3 ETS-domain transcription factor. Oncogene 17, 93–104.

Bruneau, B.G., 2002. Transcriptional regulation of vertebrate cardiac morphogenesis. Circ. Res. 90, 509–519.

Buckingham, M., Meilhac, S., Zaffran, S., 2005. Building the mammalian heart from two sources of myocardial cells. Nat. Rev. Genet. 6, 826–835.

Cai, C.L., Liang, X., Shi, Y., Chu, P.H., Pfaff, S.L., Chen, J., Evans, S., 2003. Isl1 identifies a cardiac progenitor population that proliferates prior to differentiation and contributes a majority of cells to the heart. Dev. Cell 5, 877–889.

Chen, J.N., Fishman, M.C., 1996. Zebrafish tinman homolog demarcates the heart field and initiates myocardial differentiation. Development 122, 3809–3816.

Chen, Y., Schier, A.F., 2002. Lefty proteins are long-range inhibitors of squint-mediated nodal signaling. Curr. Biol. 12, 2124–2128.

Chocron, S., Verhoeven, M.C., Rentzsch, F., Hammerschmidt, M., Bakkers, J., 2007. Zebrafish Bmp4 regulates left–right asymmetry at two distinct developmental time points. Dev. Biol. 305, 577–588.

Délot, E.C., Bahamonde, M.E., Zhao, M., Lyons, K.M., 2003. BMP signaling is required for septation of the outflow tract of the mammalian heart. Development 130, 209–220.

Dick, A., Meier, A., Hammerschmidt, M., 1999. Smad1 and Smad5 have distinct roles during dorsoventral patterning of the zebrafish embryo. Dev. Dyn. 216, 285–298.

Dick, A., Hild, M., Bauer, H., Imai, Y., Maifeld, H., Schier, A.F., Talbot, W.S., Bouwmeester, T., Hammerschmidt, M., 2000. Essential role of Bmp7 (snailhouse) and its prodomain in dorsoventral patterning of the zebrafish embryo. Development 127, 343–354.

Dunwoodie, S.L., 2007. Combinatorial signaling in the heart orchestrates cardiac induction, lineage specification and chamber formation. Semin. Cell Dev. Biol. 18, 54–66.

Frasch, M., 1995. Induction of visceral and cardiac mesoderm by ectodermal Dpp in the early Drosophila embryo. Nature 374, 464–467.

Fürthauer, M., Thisse, C., Thisse, B., 1997. A role for FGF-8 in the dorsoventral patterning of the zebrafish gastrula. Development 124, 4253–4264.

Gritsman, K., Zhang, J., Cheng, S., Heckscher, E., Talbot, W.S., Schier, A.F., 1999. The EGF-CFC protein one-eyed pinhead is essential for nodal signaling. Cell 97, 121–132.

Hild, M., Dick, A., Rauch, G.J., Meier, A., Bouwmeester, T., Haffter, P., Hammerschmidt, M., 1999. The smad5 mutation somitabun blocks Bmp2b signaling during early dorsoventral patterning of the zebrafish embryo. Development 126, 2149–2159.

Ho, R.K., Kane, D.A., 1990. Cell-autonomous action of zebrafish spt-1 mutation in specific mesodermal precursors. Nature 348, 728–730.

Hochgreb, T., Linhares, V.L., Menezes, D.C., Sampaio, A.C., Yan, C.Y., Cardoso, W.V., Rosenthal, N., Xavier-Neto, J., 2003. A caudorostral wave of RALDH2 conveys anteroposterior information to the cardiac field. Development 130, 5363–5374.

Hogan, B.M., Layton, J.E., Pyati, U.J., Nutt, S.L., Hayman, J.W., Varma, S., Heath, J.K., Kimelman, D., Lieschke, G.J., 2006. Specification of the primitive myeloid precursor pool requires signaling through Alk8 in zebrafish. Curr. Biol. 16, 506–511.

Huang, C.J., Tu, C.T., Hsiao, C.D., Hsieh, F.J., Tsai, H.J., 2003. Germ-line transmission of a myocardium-specific GFP transgene reveals critical regulatory elements in the cardiac myosin light chain 2 promoter of zebrafish. Dev. Dyn. 228, 30–40.

Keegan, B.R., Meyer, D., Yelon, D., 2004. Organization of cardiac chamber progenitors in the zebrafish blastula. Development 131, 3081–3091.

Kelly, R.G., Brown, N.A., Buckingham, M.E., 2001. The arterial pole of the mouse heart forms from Fgf10-expressing cells in pharyngeal mesoderm. Dev. Cell 1, 435–440.

Kimmel, C.B., Warga, R.M., Schilling, T.F., 1990. Origin and organization of the zebrafish fate map. Development 108, 581–594.

Kishimoto, Y., Lee, K.H., Zon, L., Hammerschmidt, M., Schulte-Merker, S., 1997. The molecular nature of zebrafish swirl: BMP2 function is essential during early dorsoventral patterning. Development 124, 4457–4466.

Klaus, A., Saga, Y., Taketo, M.M., Tzahor, E., Birchmeier, W., 2007. Distinct roles of Wnt/beta-catenin and Bmp signaling during early cardiogenesis. Proc. Natl. Acad. Sci. U. S. A. 104, 18531–18536.

Kondo, M., 2007. Bone morphogenetic proteins in the early development of zebrafish. FEBS J. 274, 2960–2967.

Lee, K.H., Evans, S., Ruan, T.Y., Lassar, A.B., 2004. SMAD-mediated modulation of YY1 activity regulates the BMP response and cardiac-specific expression of a GATA4/5/6-dependent chick Nkx2.5 enhancer. Development 131, 4709–4723.

Liberatore, C.M., Searcy-Schrick, R.D., Vincent, E.B., Yutzey, K.E., 2002. Nkx-2.5 gene induction in mice is mediated by a Smad consensus regulatory region. Dev. Biol. 244, 243–256.

Lien, C.L., McAnally, J., Richardson, J.A., Olson, E.N., 2002. Cardiac-specific activity of an Nkx2-5 enhancer requires an evolutionarily conserved Smad binding site. Dev. Biol. 244, 257–266.

Liu, W., Selever, J., Wang, D., Lu, M.F., Moses, K.A., Schwartz, R.J., Martin, J.F., 2004. Bmp4 signaling is required for outflow-tract septation and branchial-arch artery remodeling. Proc. Natl. Acad. Sci. U. S. A. 101, 4489–4494.

Mably, J.D., Mohideen, M.A., Burns, C.G., Chen, J.N., Fishman, M.C., 2003. heart of glass regulates the concentric growth of the heart in zebrafish. Curr. Biol. 13, 2138–2147.

Marques, S.R., Lee, Y., Poss, K.D., Yelon, D., 2008. Reiterative roles for FGF signaling in the establishment of size and proportion of the zebrafish heart. Dev. Biol. 321, 397–406.

Martínez-Barberá, J.P., Toresson, H., Da Rocha, S., Krauss, S., 1997. Cloning and expression of three members of the zebrafish Bmp family: Bmp2a, Bmp2b and Bmp4. Gene 198, 53–59.

Meilhac, S.M., Esner, M., Kelly, R.G., Nicolas, J.F., Buckingham, M.E., 2004. The clonal origin of myocardial cells in different regions of the embryonic mouse heart. Dev. Cell 6, 685–698.

Mine, N., Anderson, R.M., Klingensmith, J., 2008. BMP antagonism is required in both the node and lateral plate mesoderm for mammalian left–right axis establishment. Development 135, 2425–2434.

Mintzer, K.A., Lee, M.A., Runke, G., Trout, J., Whitman, M., Mullins, M.C., 2001. Lost-a-fin encodes a type I BMP receptor, Alk8, acting maternally and zygotically in dorsoventral pattern formation. Development 128, 859–869.

Moorman, A.F., Christoffels, V.M., 2003. Cardiac chamber formation: development, genes, and evolution. Physiol. Rev. 83, 1223–1267.

Müller, F., Blader, P., Rastegar, S., Fischer, N., Knöchel, W., Strähle, U., 1999. Characterization of zebrafish smad1, smad2 and smad5: the amino-terminus of smad1 and smad5 is required for specific function in the embryo. Mech. Dev. 88, 73–88.

Mullins, M.C., Hammerschmidt, M., Kane, D.A., Odenthal, J., Brand, M., van Eeden, F.J., Furutani-Seiki, M., Granato, M., Haffter, P., Heisenberg, C.P., Jiang, Y.J., Kelsh, R.N., Nüsslein-Volhard, C., 1996. Genes establishing dorsoventral pattern formation in the zebrafish embryo: the ventral specifying genes. Development 123, 81–93.

Nakajima, Y., Yamagishi, T., Ando, K., Nakamura, H., 2002. Significance of bone morphogenetic protein-4 function in the initial myofibrillogenesis of chick cardiogenesis. Dev. Biol. 245, 291–303.

Nguyen, V.H., Schmid, B., Trout, J., Connors, S.A., Ekker, M., Mullins, M.C., 1998. Ventral and lateral regions of the zebrafish gastrula, including the neural crest progenitors, are established by a bmp2b/swirl pathway of genes. Dev. Biol. 199, 93–110.

Nusslein-Volhard, C., Dahm, R., 2002. Zebrafish, A Practical Approach. Oxford University Press.

Parker, L., Stainier, D.Y., 1999. Cell-autonomous and non-autonomous requirements for the zebrafish gene cloche in hematopoiesis. Development 126, 2643–2651.

Prall, O.W., Menon, M.K., Solloway, M.J., Watanabe, Y., Zaffran, S., Bajolle, F., Biben, C., McBride, J.J., Robertson, B.R., Chaulet, H., Stennard, F.A., Wise, N., Schaft, D., Wolstein, O., Furtado, M.B., Shiratori, H., Chien, K.R., Hamada, H., Black, B.L., Saga, Y., Robertson, E.J., Buckingham, M.E., Harvey, R.P., 2007. An Nkx2-5/Bmp2/Smad1 negative feedback loop controls heart progenitor specification and proliferation. Cell 128, 947–959.

Pyati, U.J., Webb, A.E., Kimelman, D., 2005. Transgenic zebrafish reveal stage-specific roles for Bmp signaling in ventral and posterior mesoderm development. Development 132, 2333–2343.

Pyati, U.J., Cooper, M.S., Davidson, A.J., Nechiporuk, A., Kimelman, D., 2006. Sustained Bmp signaling is essential for cloaca development in zebrafish. Development 133, 2275–2284.

Reifers, F., Walsh, E.C., Léger, S., Stainier, D.Y., Brand, M., 2000. Induction and differentiation of the zebrafish heart requires fibroblast growth factor 8 (fgf8/acerebellar). Development 127, 225–235.

Reiter, J.F., Verkade, H., Stainier, D.Y., 2001. Bmp2b and Oep promote early myocardial differentiation through their regulation of gata5. Dev. Biol. 234, 330–338.

Rohr, S., Otten, C., Abdelilah-Seyfried, S., 2008. Asymmetric involution of the myocardial field drives heart tube formation in zebrafish. Circ. Res. 102, e9–e12.

Schlange, T., Andrée, B., Arnold, H.H., Brand, T., 2000. BMP2 is required for early heart development during a distinct time period. Mech. Dev. 91, 259–270.

Schoenebeck, J.J., Keegan, B.R., Yelon, D., 2007. Vessel and blood specification override cardiac potential in anterior mesoderm. Dev. Cell 13, 254–267.

Schultheiss, T.M., Burch, J.B., Lassar, A.B., 1997. A role for bone morphogenetic proteins in the induction of cardiac myogenesis. Genes Dev. 11, 451–462.

Scott, I.C., Masri, B., D'Amico, L.A., Jin, S.W., Jungblut, B., Wehman, A.M., Baier, H., Audigier, Y., Stainier, D.Y., 2007. The g protein-coupled receptor agtrl1b regulates early development of myocardial progenitors. Dev. Cell 12, 403–413.

Shi, Y., Katsev, S., Cai, C., Evans, S., 2000. BMP signaling is required for heart formation in vertebrates. Dev. Biol. 224, 226–237.

Smith, K.A., Chocron, S., von der Hardt, S., de Pater, E., Soufan, A., Bussmann, J., Schulte-Merker, S., Hammerschmidt, M., Bakkers, J., 2008. Rotation and asymmetric development of the zebrafish heart requires directed migration of cardiac progenitor cells. Dev. Cell 14, 287–297.

Solloway, M.J., Robertson, E.J., 1999. Early embryonic lethality in Bmp5;Bmp7 double mutant mice suggests functional redundancy within the 60A subgroup. Development 126, 1753–1768.

Stainier, D.Y., Lee, R.K., Fishman, M.C., 1993. Cardiovascular development in the zebrafish. I. Myocardial fate map and heart tube formation. Development 119, 31–40.

Stickney, H.L., Imai, Y., Draper, B., Moens, C., Talbot, W.S., 2007. Zebrafish bmp4 functions during late gastrulation to specify ventroposterior cell fates. Dev. Biol. 310, 71–84.

Stottmann, R.W., Choi, M., Mishina, Y., Meyers, E.N., Klingensmith, J., 2004. BMP receptor IA is required in mammalian neural crest cells for development of the cardiac outflow tract and ventricular myocardium. Development 131, 2205–2218.

Sugi, Y., Yamamura, H., Okagawa, H., Markwald, R.R., 2004. Bone morphogenetic protein-2 can mediate myocardial regulation of atrioventricular cushion mesenchymal cell formation in mice. Dev. Biol. 269, 505–518.

Thomas, N.A., Koudijs, M., van Eeden, F.J., Joyner, A.L., Yelon, D., 2008. Hedgehog signaling plays a cell-autonomous role in maximizing cardiac developmental potential. Development 135, 3789–3799.

Tucker, J.A., Mintzer, K.A., Mullins, M.C., 2008. The BMP signaling gradient patterns dorsoventral tissues in a temporally progressive manner along the anteroposterior axis. Dev. Cell 14, 108–119.

van Wijk, B., Moorman, A.F., van den Hoff, M.J., 2007. Role of bone morphogenetic proteins in cardiac differentiation. Cardiovasc. Res. 74, 244–255.

von der Hardt, S., Bakkers, J., Inbal, A., Carvalho, L., Solnica-Krezel, L., Heisenberg, C.P., Hammerschmidt, M., 2007. The Bmp gradient of the zebrafish gastrula guides migrating lateral cells by regulating cell–cell adhesion. Curr. Biol. 17, 475–487.

Waxman, J.S., Keegan, B.R., Roberts, R.W., Poss, K.D., Yelon, D., 2008. Hoxb5b acts downstream of retinoic acid signaling in the forelimb field to restrict heart field potential in zebrafish. Dev. Cell 15, 923–934.

Wieser, R., Wrana, J.L., Massagué, J., 1995. GS domain mutations that constitutively activate T beta R-I, the downstream signaling component in the TGF-beta receptor complex. EMBO J. 14, 2199–2208.

Xavier-Neto, J., Rosenthal, N., Silva, F.A., Matos, T.G., Hochgreb, T., Linhares, V.L., 2001. Retinoid signaling and cardiac anteroposterior segmentation. Genesis 31, 97–104.

Yelick, P.C., Abduljabbar, T.S., Stashenko, P., 1998. zALK-8, a novel type I serine/threonine kinase receptor, is expressed throughout early zebrafish development. Dev. Dyn. 211, 352–361.

Yelon, D., Horne, S.A., Stainier, D.Y., 1999. Restricted expression of cardiac myosin genes reveals regulated aspects of heart tube assembly in zebrafish. Dev. Biol. 214, 23–37.

Yelon, D., Ticho, B., Halpern, M.E., Ruvinsky, I., Ho, R.K., Silver, L.M., Stainier, D.Y., 2000. The bHLH transcription factor hand2 plays parallel roles in zebrafish heart and pectoral fin development. Development 127, 2573–2582.

Yin, Z., Frasch, M., 1998. Regulation and function of tinman during dorsal mesoderm induction and heart specification in *Drosophila*. Dev. Genet. 22, 187–200.

Yu, P.B., Hong, C.C., Sachidanandan, C., Babitt, J.L., Deng, D.Y., Hoyng, S.A., Lin, H.Y., Bloch, K.D., Peterson, R.T., 2008. Dorsomorphin inhibits BMP signals required for embryogenesis and iron metabolism. Nat. Chem. Biol. 4, 33–41.

Zaffran, S., Frasch, M., 2002. Early signals in cardiac development. Circ. Res. 91, 457–469.

Zeng, X.X., Wilm, T.P., Sepich, D.S., Solnica-Krezel, L., 2007. Apelin and its receptor control heart field formation during zebrafish gastrulation. Dev. Cell 12, 391–402.

Zhang, H., Bradley, A., 1996. Mice deficient for BMP2 are nonviable and have defects in amnion/chorion and cardiac development. Development 122, 2977–2986.